

Electronic structure of superoxygenated La_2NiO_4 domains with ordered oxygen interstitials

Thomas Jarlborg^{1,2} and Antonio Bianconi^{2,3,4}

¹*DPMC, University of Geneva, 24 Quai Ernest-Ansermet, CH-1211 Geneva 4, Switzerland*

²*RICMASS Rome International Center for Materials Science Superstripes, Via dei Sabelli 119A, 00185 Rome, Italy*

³*Institute of Crystallography, Consiglio Nazionale delle Ricerche, via Salaria, 00015 Monterotondo, Italy*

⁴*INSTM, Consorzio Interuniversitario Nazionale per la Scienza e Tecnologia dei Materiali, Udr Rome, Italy*

The electronic structures of $\text{La}_2\text{NiO}_{4+\delta}$, where additional oxygen interstitials are forming stripes along (1,1,0), are presented. Spin-polarized calculations show that ferromagnetism on Ni sites is reduced near the stripes and enhanced far from the stripes. Totally the magnetic moment becomes reduced because of oxygen interstitials. It is suggested that the oxygen interstitial concentration in oxygen rich domains in nickelates suppress magnetism and give multiband metallic domains.

PACS numbers: 74.20.Pq, 74.72.-h, 74.25.Jb

I. INTRODUCTION.

Superoxygenated $\text{La}_2\text{NiO}_{4+\delta}$ is an oxygen ionic conductor at high temperature [1–6] with interesting electrochemical, thermo-mechanical properties and applications in fuel cells [7–10]. The gas of mobile oxygen interstitials (O_i) at high temperature freeze below about 400K forming crystalline grains, as is observed by electron and neutron diffraction [11–15]. At lower temperature, below 200K, the electronic structure shows the onset of spin and charge stripes i.e., one dimensional spin density waves (SDW) and charge density waves (CDW) [16–20] due to ordering of polarons [21]. Localized charges trapped by local lattice distortions (LLD) make periodic lattice distortions (PLD), as obtained by doping a magnetic Mott insulator La_2NiO_4 . The polaronic CDW in $\text{La}_2\text{NiO}_{4+\delta}$ is therefore a model system to be compared with the more complex case in doped cuprates where polarons [22–24] coexist with free carriers [25–27] giving origin to Feshbach like resonances of polaron pairs and BCS pairs [28–32] in the superconducting phase. The other common feature of nickelates and cuprates is the electronic phase separation in multi-orbital strongly correlated systems which is predicted by the multiband Hubbard model in presence of long range Coulomb interaction [33, 34]. The stripe inhomogeneity of the lattice due to i) ordering of oxygen interstitials in ordered domains [35] ii) oxygen mobility at high temperature and the electron-lattice interaction at low temperature in nickelates and cuprates is controlled by the lattice mismatch between the CuO_2 or NiO_2 2D atomic layers and the $\text{La}_2\text{O}_{2+\delta}$ blocks layers. [36, 37] which is key feature for the lattice stripes phase in cuprates [38, 39].

$\text{La}_2\text{NiO}_{4+\delta}$ is isostructural with the widely studied $\text{La}_2\text{CuO}_{4+\delta}$ which could make its band structure very similar to optimally doped La_2CuO_4 (LCO) [40, 41], even if the band filling is different. Ordering of excess oxygens in interstitial positions in LCO will also enhance T_c [35], and the Fermi surface (FS) is shown to become fragmented by the oxygens [42]. Moreover it is similar with other systems where oxygen interstitials like in

$\text{HgBa}_2\text{CuO}_{4+\delta}$ or oxygen vacancies like in $\text{Ba}_2\text{CuO}_{4-\delta}$ increases considerably T_c [43–45]. The electronic structure of oxygenated nickelates $\text{La}_2\text{NiO}_{4+\delta}$ is not known. For instance it is not established that ferromagnetism (FM) can be suppressed and allow for superconductivity in these materials. The equivalence of spin-phonon coupling in the cuprates, where phonons can enforce spin waves [46], is not known. It can lead to fluctuations of local moment amplitudes as in other FM materials [47, 48]. Therefore it is of high interest to calculate the electronic structure of the domains present in $\text{La}_2\text{NiO}_{4+\delta}$ below 400K with a stoichiometric content of oxygen interstitials. In this work we present electronic structure results for the highly hole doped puddles of oxygen interstitials in superoxygenated La_2NiO_4 , ordered into stripes along (1,1,0) mostly separated by 3 unitcells. The method of calculation is presented in sect. II. Experimental information on oxygen ordering is used to define the supercells of O-rich LNO, as discussed in sect. II. In sect. III we discuss the results of the calculations, and some ideas for future works are given together with the conclusions in sect. IV.

II. METHOD OF CALCULATION.

The calculations are made using the linear muffin-tin orbital (LMTO) method [49, 50] and the local spin-density approximation (LSDA) [51]. The details of the methods have been published earlier [42], [52]–[56]. The elementary cell of La_2NiO_4 (LNO) contains La sites at (0,0, $\pm 0.721c$), Ni at (0,0,0), planar O's at (0.5,0,0) and (0, ± 0.5 ,0) and apical O's at (0,0, $\pm 0.366c$), in units of the lattice constant $a_0=3.86 \text{ \AA}$, where $c=1.16$. In addition to the MT-spheres at the atomic sites we insert MT-spheres at positions (± 0.5 ,0, $\pm 0.5c$) and (0, ± 0.5 , $\pm 0.5c$) to account for the positions of empty spheres.

The atomic sphere radii are 1.75 \AA (La), 1.25 \AA (Cu), 1.17 \AA (planar oxygens, oxygen, interstitials, O_i , and empty spheres), and 1.20 \AA (apical oxygens), respectively. Six units of the elementary cell La_2NiO_4 are

TABLE I: Decomposition of the total DOS at E_F on each of the six Ni atoms in $\text{La}_{12}\text{Ni}_6\text{O}_{25}$ (LNO-1) and $\text{La}_{12}\text{Ni}_6\text{O}_{24}$ (LNO-0) (in units of $(\text{cell} \cdot \text{eV})^{-1}$), magnetic moment per site, m , (μ_B per site), and number of valence electrons per Ni site, Q . The total magnetic moment in the LNO-0 cell is $1.32 \mu_B$ and in LNO-1 $0.76 \mu_B$. The interstitial site in LNO-1 is at the y -layer between site 1 and 2.

	1	2	3	4	5	6	in LNO-0
$N(E_F)$	1.2	1.6	2.4	2.6	2.4	1.6	1.9
m	0	-0.03	0.20	0.25	0.19	-0.02	0.18
Q	9.09	9.10	9.11	9.12	9.11	9.10	9.15

TABLE II: The local decomposition of the DOS at E_F on the different Ni atoms in $\text{La}_{16}\text{Ni}_8\text{O}_{33}$ (LNO8-1) and $\text{La}_{16}\text{Ni}_8\text{O}_{34}$ (LNO8-2). The last column shows the total DOS per cell, all in units of $(\text{cell} \cdot \text{eV})^{-1}$. Site 1 is nearest to the oxygen interstitials, site 5 is most distant, and the other sites are counted pairwise as function of increasing distance from the O-rich layer.

cell	1	± 2	± 3	± 4	5	total
LNO8-1 $N(E_F)$	0.8	1.3	1.9	2.4	2.7	25
LNO8-2 $N(E_F)$	1.3	1.0	1.3	1.8	2.3	20

put together to form a long supercell, $\text{La}_{12}\text{Ni}_6\text{O}_{24}$, with the generating lattice vectors $(1, -1, 0)$, $(3, 3, 0)$, and $(.5, .5, c)$, so that its axis is oriented parallel to the $(1, 1, 0)$ -direction, i.e. at 45 degrees from the Ni-O bond direction along $(1, 0, 0)$. The band calculations are made for this supercell containing 54 sites totally, where one of

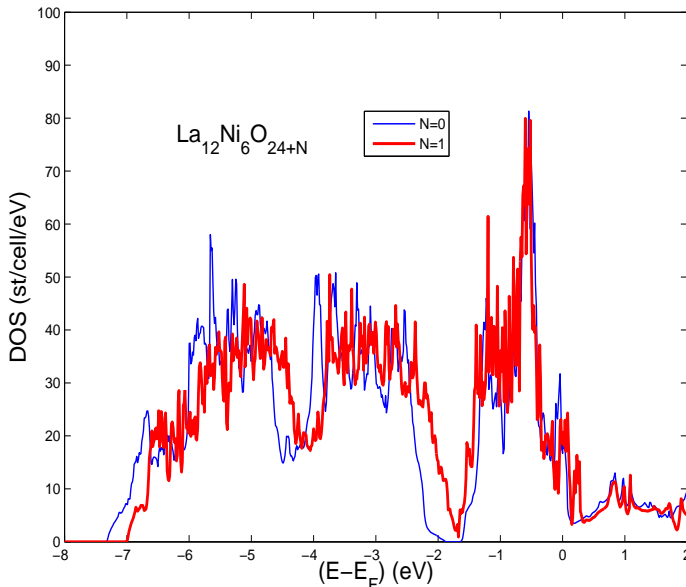


FIG. 1: (Color online) The total DOS for $\text{La}_{12}\text{Ni}_6\text{O}_{24+N}$ with $N=0$ and $N=1$.

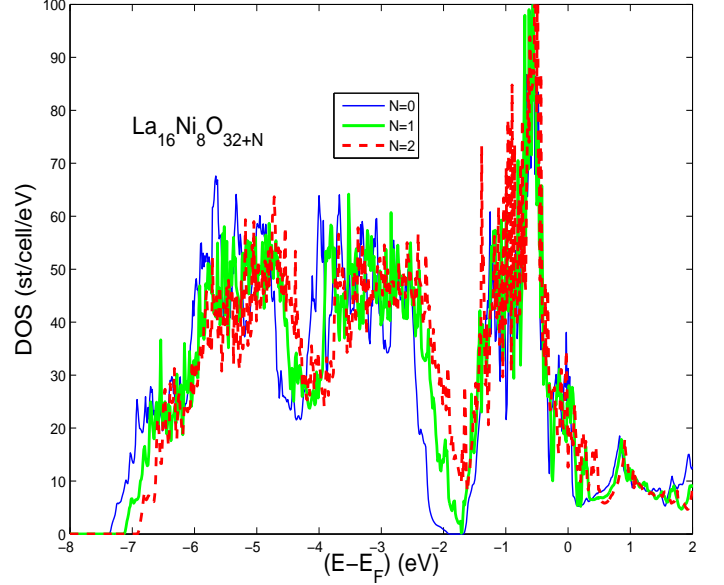


FIG. 2: (Color online) The total DOS for $\text{La}_{16}\text{Ni}_8\text{O}_{32+N}$ with $N=0, 1$ and 2 .

the empty sites at the interstitial positions is occupied by the excess oxygen ion. These supercells are chosen in order to represent fairly well the experimentally determined structures [57]. The basis set goes up through $\ell=2$ for all sites. The z-projected IBZ (irreducible Brillouin zone) corresponding to the supercell is shown in Fig. 3 by the limits $\Gamma - M_3 - X_3 - R$. It corresponds to one third (folded) BZ for antiferromagnetic (AFM) LCO. Paramagnetic and spin-polarized calculations are made for these cells. Self-consistency is made with 192 k-points and final results are based on 702 points in the IBZ.

No interstitial sites are occupied with O in one set of the calculations (called LNO-0). The LNO-0 results serve as a reference for comparison with the results with oxygen interstitials. For instance, the FS for (undoped) LNO forms a circle centered at the Γ point in BZ of the elementary cell, but since the BZ corresponding to the supercell is folded and very flat along $(1, 1, 0)$ it is necessary to identify the circle from several FS pieces in the folded zone. In the second set of calculations we insert one oxygen ($\text{La}_{12}\text{Ni}_6\text{O}_{24+1}$, LNO-1) at an interstitial position to calculate the electronic structure of a $\text{La}_2\text{NiO}_{4.166}$ domain.

Paramagnetic calculations were also made for $\text{La}_{16}\text{Ni}_8\text{O}_{32+N}$ by putting together 8 elementary cells of La_2NiO_4 to calculate the electronic structure of a $\text{La}_2\text{NiO}_{4.125}$ domain. Totally there are 72 sites in these supercells, and $N = 0, 1$ or 2 interstitial oxygens are inserted (LNO8-0, LNO8-1 and LNO8-2, respectively). These cells are of equivalent size as the cells that was used for the studies of electronic structures of interstitial O in LCO [42], which is helpful for direct comparisons between the nickelates and cuprates. An important

difference between LNO and LCO is that there is one less filled d-band per metal atom. In the largest cell of LNO8-0 there are 208 occupied bands, in LCO8-0 there are 212. Here, for LNO we concentrate the investigations of the shorter cells, since they correspond best to the experimentally found periodicity of O-interstitials in LNO [11–15].

The excess O_i 's sit at the interstitial interlayer positions, above the oxygen ion in the NiO_2 plane of the orthorhombic unit cell. The insertion of O_i 's is expected to induce hole doping, because each new oxygen interstitial will bring 4 new bands well below E_F (one "s" and 3 "p"), but the oxygen has only 2 "s" and 4 "p" electrons. Therefore, simple arguments suggest that one Ni-O band becomes unfilled, i.e. E_F has to go down relative to the rest of the bands. However, other atoms like La serve as charge reservoirs, lattice reconstructions are likely, and in addition the excess O positions are ordered in stripe-like patterns like in $La_2CuO_{4+\delta}$ [57].

Correlation is not expected to be an issue for cuprates and nickelates with hole doping larger than 0.2 holes per Cu (or Ni) site away from half-filling of the d-band. This is confirmed for cuprates from ARPES (angular-resolved photoemission spectroscopy) and ACAR (angular correlation of positron annihilation radiation), which detect FS's and bands that evolves with doping larger than 0.2 holes per Cu site in agreement with DFT (density-functional theory) calculations [58–60].

III. RESULTS AND DISCUSSION.

The nonmagnetic (NM) total DOS at the Fermi level for $La_{12}Ni_6O_{24+N}$ and $La_{16}Ni_8O_{32+N}$ is shown in Figs. 1-2. It can be seen from the partial gap 1.5-2 eV below E_F that the band filling decreases when one (or two) oxygen interstitials (O_i) are added in form of stripes. In contrast to LCO [42] there is no clear variation of the total $N(E_F)$ as function of the number of O_i . The total $N(E_F)$ in LNO-0 and LNO-1, are comparable; both about 19 ($cell \cdot eV$)⁻¹, and in LNO8-0, LNO8-1 and LNO8-2 about 26, 25 and 20 ($cell \cdot eV$)⁻¹. Also in contrast to LCO, there is no strikingly high $N(E_F)$ on the interstitial oxygen sites. The local DOS on Ni-sites near and far from the interstitial site are very different as shown in Tables I. The same trends are found for the larger LNO8-cells, see Table II. The DOS at E_F on Ni-sites nearest to the interstitial O are lower than the average, while in the region far from the interstitials the $N(E_F)$ values are significantly larger than for Ni in LNO-0. However, this local distribution of the Ni-DOS is delicate: at 0.25-0.30 eV above E_F the distribution is reversed so that local DOS is peaked ($\sim 3(cell \cdot eV)^{-1}$) nearest to O_i , and it goes down rapidly for the next layers, and reaches $\sim 0.5(cell \cdot eV)^{-1}$ on the most distant Ni site. The differences in local $N(E_F)$ are also reflected in the local moments on Ni, as can be expected from the DOS at E_F and the criterion for Stoner magnetism. Ferromagnetism (FM) tends to disappear

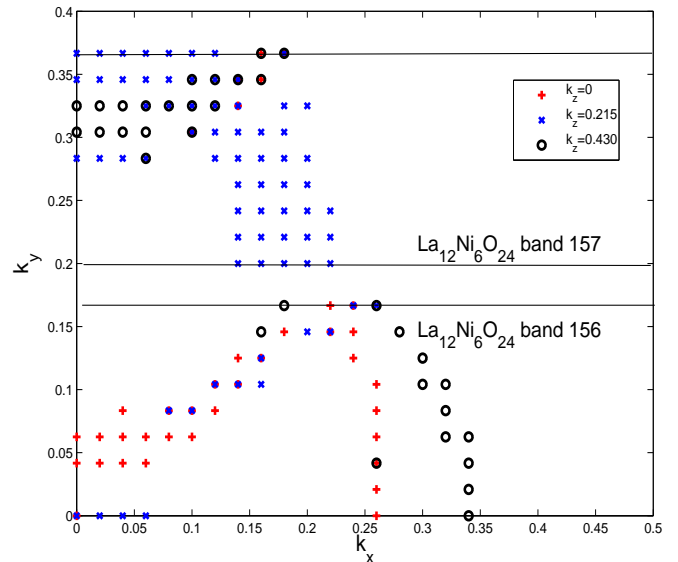


FIG. 3: (Color online) Upper panel: The Fermi surface of band 157 (upper panel) and band 156 (lower panel) for non-magnetic $La_{12}Ni_6O_{24}$ indicated by k -points (k_x, k_y, k_z) for which $E(K)$ is within 0.01 eV from E_F . The different marks indicate three different levels of k_z . The limits of the rectangular IBZ of the supercell given by the rectangle Γ -M₃-X₃-R. Unfolding the FS of band 156 leads to circular FS within the IBZ elementary cell.

near layers with interstitial O. The moment on the Ni close to the O_i -site is practically zero, and in the next Ni layers the moments are even slightly negative. Further away the moments become clearly FM again, and their amplitude are even larger (0.2-0.25 μ_B) than the moment per Ni-site in undoped LNO (0.18 μ_B). The obvious question is whether FM in nickelates is responsible for the absence of superconductivity in LNO. However, the domains with increased O_i -concentrations made of ordered O_i -stripes show weaker FM, but they are still metallic with a different multiband FS from what is found in LCO superconductors.

The main difference between LCO and LNO with oxygen interstitials, is due to the fact that Ni has one electron less than Cu. Thus, LNO is like a heavily hole doped version of LCO with E_F pushed down within the high DOS of the 3d-bands. This makes the DOS large in undoped LNO, sufficiently large for Stoner magnetism, while this is not the case in LCO [53]. The changes of the effective charges (see Table I) show a weak hole doping on Ni when the number of O_i increases. The same trend is found in the LNO8 results, and it is in agreement with the behavior for LCO.

In Figs. 3-4 are displayed the FS pieces in different k_z -planes of the irreducible BZ for LNO-0 and LNO-1, respectively. For the calculations without oxygen interstitial it is easy to recognize simple Γ -centered FS circles in the unfolded BZ, as for LCO [42]. There are minor

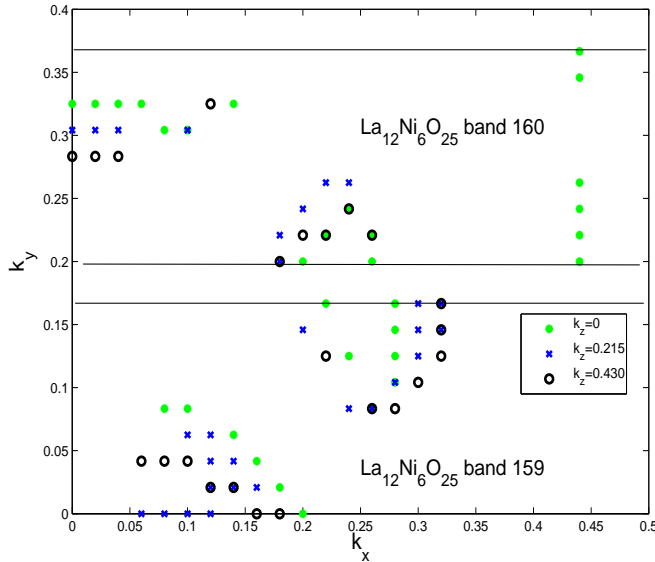


FIG. 4: (Color online) The FS of $\text{La}_{12}\text{Ni}_6\text{O}_{24+1}$ displayed as in Fig. 3.

modifications in different k_z planes because of a weak 3-D dispersion. The diameter of the circles is smaller than in undoped LCO. As for stripes in LCO, the FS's become segmented and show gaps when there are O_i stripes, and

it becomes more difficult to visualize their projection in an unfolded zone.

IV. CONCLUSION.

Oxygen interstitials forming of atomic stripes in the spacer layers form three overlapping mini-bands crossing E_F making the local Ni-d DOS larger on sites far from the O_i -stripes. Near the stripes the local Ni-d DOS is reduced. The consequence is that FM is enhanced between the stripes and almost quenched at the stripes. Thus, the natural growth of O_i -stripes in the oxygen rich domains seems to be an efficient way to suppress FM in the nickelate, and if the method can be optimized it might be a path for making the nickelates good metals. It can be noted that suppression of FM is one of the requirements for superconductivity. The band structures in LNO and LCO are different because of the different band filling, but the evolution of the FS's in undoped and oxygenated LNO behave quite similarly as in LCO. The undoped material has simple FS's much like the ones for supercells of stoichiometric LCO despite the large differences of d-band filling between Cu and Ni. Finally we have shown that oxygen interstitials order breaks up the FS's into fragments with gaps in between, similar to the process in oxygenated LCO [42].

-
- [1] S. Y. Jeon, M. B. Choi, H. N. Im, J. H. Hwang, and S. J. Song, *Journal of Physics and Chemistry of Solids* **73**, 656 (2012).
 - [2] Z. Li, R. Haugrud, and T. Norby, *Solid State Ionics* **184**, 42 (2011).
 - [3] A. Chroneos, R. V. Vovk, I. L. Goulatis, and L. I. Goulatis, *Journal of Alloys and Compounds* 494, 190 (2010).
 - [4] M. Burriel, G. Garcia, J. Santiso, J. A. Kilner, R. J. Chater, and S. J. Skinner, *J. Mater. Chem.* **18**, 416 (2008).
 - [5] V. V. Kharton, A. P. Viskup, E. N. Naumovich and F. M. B. Marques, *J. Mater. Chem.* **9**, 2623 (1999).
 - [6] A. Chroneos, D. Parfitt, J. A. Kilner, and R. W. Grimes, *J. Mater. Chem.* 20, 266 (2010).
 - [7] L. Lu, Y. Guo, H. Zhang, and J. Jin, *temperature solid oxide fuel cells Materials Research Bulletin* 45, 1135 (2010).
 - [8] B. X. Huang, J. Malzbender, R. W. Steinbrech *Journal of Materials Science* **46**, 4937-4941 (2011).
 - [9] S. Y. Jeon, M. B. Choi, J. H. Hwang, E. D. Wachsman, and S.-J. Song, *Journal of Solid State Electrochemistry* **16**, 785 (2012).
 - [10] A. M. Hernandez, L. Moggi, and A. Caneiro, *International Journal of Hydrogen Energy* **35**, 6031 (2010).
 - [11] Z. Hiroi, T. Obata, M. Takano, Y. Bando, Y. Takeda, and O. Yamamoto, *Physical Review B* **41**, 11665 (1990).
 - [12] M. Sayagues, M. Vallet-Regi, J. L. Hutchison, and J. M. Gonzalez-Calbet, *Journal of Solid State Chemistry* **125**, 133 (1996).
 - [13] W. Paulus, A. Cousson, G. Dhalenne, J. Berthon, A. Revcolevschi, S. Hosoya, W. Treutmann, G. Heger, and R. Le Toquin, *Solid State Sciences* 4, 565 (2002).
 - [14] M. Huecker, K. Chung, M. Chand, T. Vogt, J. M. Tranquada, and D. J. Buttrey, *Physical Review B* **70**, 064105 (2003).
 - [15] T. Klande, K. Efimov, S. Cusenza, K.-D. Becker, and A. Feldhoff, *Journal of Solid State Chemistry* **184**, 3310 (2011).
 - [16] I. M. Abu-Shiekh, O. Bakharev, H. B. Brom, and J. Zaanen, *Physical Review Letters* **87**, 237201 (2001).
 - [17] C. C. Homes and J. M. Tranquada, *Physical Review B* **75** 045128 (2007).
 - [18] J. M. Tranquada, J. E. Lorenzo, D. J. Buttrey, and V. Sachan, *Physical Review B* **52**, 3581 (1995).
 - [19] N. Poirot, R. A. Souza, and C. M. Smith, *Solid State Sciences* **13**, 1494 (2011).
 - [20] N. Poirot, V. T. Phuoc, G. Gruener, and F. Gervais, *Solid State Sciences* **7**, 1157 (2005).
 - [21] J. Zaanen, P. Littlewood *Physical Review B* **50**, 7222 (1994). doi:10.1103/physrevb.50.7222
 - [22] A. Bianconi, M. Missori, H. Oyanagi, H. Yamaguchi, Y. Nishihara, and S. Della Longa, *EPL (Europhysics Letters)* **31**, 411 (1995).
 - [23] A. Bianconi and M. Missori, *Solid State Communications* **91**, 287 (1994).
 - [24] A. Bianconi, *Physica C* **235-240**, 269 (1994).

- [25] A. Bianconi, D. Di Castro, G. Bianconi, A. Pifferi, N. L. Saini, F. C. Chou, D. C. Johnston, and M. Colapietro, *Physica C: Superconductivity* **341**, 1719 (2000).
- [26] A. Bianconi, *International Journal of Modern Physics B* **14**, 3289 (2000).
- [27] N. Poccia, A. Ricci, G. Campi, M. Fratini, A. Puri, D. Di Gioacchino, A. Marcelli, M. Reynolds, M. Burghammer, N. L. Saini, et al., *Proceedings of the National Academy of Sciences* **109**, 15685 (2012).
- [28] A. Bianconi, A. Valletta, A. Perali, and N. L. Saini, *Solid State Communications* **102**, 369 (1997).
- [29] A. Bianconi, *Journal of Superconductivity* **18**, 625 (2005).
- [30] M. Fratini, N. Poccia, and A. Bianconi, *Journal of Physics: Conference Series* **108**, 012036 (2008).
- [31] A. Bianconi, *Journal of Physics: Conference Series* **449**, 012002 (2013).
- [32] A. Bianconi, *Nature Physics* **9**, 536 (2013).
- [33] K. I. Kugel, A. L. Rakhmanov, A. O. Sboychakov, N. Poccia, and A. Bianconi, *Phys. Rev. B* **78**, 165124 (2008).
- [34] A. Bianconi, N. Poccia, A. O. Sboychakov, A. L. Rakhmanov, and K. I. Kugel, *Superconductor Science and Technology* **28**, 024005 (2015).
- [35] N. Poccia, M. Fratini, A. Ricci, G. Campi, L. Barba, A. Vittorini-Orgeas, G. Bianconi, G. Aeppli, and A. Bianconi, *Nature Materials* **10**, 733 (2011).
- [36] D. Di Castro, G. Bianconi, M. Colapietro, A. Pifferi, N. L. Saini, S. Agrestini, and A. Bianconi, *The European Physical Journal B - Condensed Matter and Complex Systems* **18**, 617 (2000).
- [37] A. Bianconi, S. Agrestini, G. Bianconi, D. Di Castro, and N. L. Saini, *Journal of Alloys and Compounds* **317-318**, 537 (2001).
- [38] J. C. Phillips, *Journal of Superconductivity and Novel Magnetism* **27**, 345 (2014).
- [39] G. Campi et al. *Nature* (2015) in press
- [40] T. Jarlborg, B. Barbiellini, R.S. Markiewicz and A. Bansil, *Phys. Rev. B* **86**, 235111, (2012).
- [41] T. Jarlborg, A. Bianconi, B. Barbiellini, R.S. Markiewicz, A. Bansil, *J. Supercond. Nov. Magn.* **26**, 2597 (2013).
- [42] T. Jarlborg and A. Bianconi, *Phys. Rev. B* **87**, 054514, (2013).
- [43] W.B. Gao, Q.Q. Liu, L.X. Yang, Y. Yu, F.Y. Li, C.Q. Jin and S. Uchida, *Phys. Rev. B* **80**, 094523 (2009)
- [44] T.H. Geballe and M. Marezio, *Physica C* **469**, 680, (2009).
- [45] O. Chmaissem, I. Grigoraviciute, H. Yamauchi, M. Karpinen and M. Marezio, *Phys. Rev. B* **82**, 104570, (2010).
- [46] T. Jarlborg, *Physica C* **454**, 5, (2007).
- [47] T. Jarlborg, *Phys. Rev.* **B89**, 184426 (2014).
- [48] T. Jarlborg, *Phys. Rev.* **B59**, 15002, (1999).
- [49] O.K. Andersen, *Phys. Rev.* **B12**, 3060 (1975).
- [50] B. Barbiellini, S.B. Dugdale and T. Jarlborg, *Comput. Mater. Sci.* **28**, 287 (2003).
- [51] O. Gunnarsson and B.I. Lundquist, *Phys. Rev. B* **13**, 4274 (1976).
- [52] T. Jarlborg, *Phys. Rev.* **B64**, 060507(R), (2001).
- [53] B. Barbiellini and T. Jarlborg, *Phys. Rev. Lett.* **101**, 157002, (2008).
- [54] T. Jarlborg, *Phys. Rev.* **B76**, 140504(R), (2007).
- [55] T. Jarlborg, *Appl. Phys. Lett.* **94**, 212503, (2009).
- [56] T. Jarlborg, *Phys. Rev.* **B84**, 064506, (2011).
- [57] M. Fratini, N. Poccia, A. Ricci, G. Campi, M. Burghammer, G. Aeppli, and A. Bianconi, *Nature* **466**, 841 (2010).
- [58] B. Barbiellini, P. Genoud, J.Y. Henry, L. Hoffmann, T. Jarlborg, A.A. Manuel, S. Massidda, M. Peter, W. Sadowski, H.J. Scheel, A. Shukla, A.K. Singh and E. Walker, *Phys. Rev. B* **43**, 7810 (1991).
- [59] W.E. Pickett, *Rev. Mod. Phys.* **61**, 433 (1989).
- [60] A. Damascelli, Z.-X. Shen and Z. Hussain, *Rev. Mod. Phys.* **75**, 473, (2003).